Journal of Bioenergetics and Biomembranes, Vol. 30, No. 1, 1998

Redox Bohr Effects (Cooperative Coupling) and the Role of Heme *a* in the Proton Pump of Cytochrome *c* Oxidase

Sergio Papa[1] and Nazzareno Capitanio[1]

Received August 20, 1997; accepted September 16, 1997

1. INTRODUCTION

Based on the principle of cooperative thermodynamic linkage of solute binding at separate sites in allosteric proteins (Wyman, 1968) and the observation of linkage between electron transfer at the metals and protolytic events (p*K* shifts) in cytochromes (Clark, 1960), Papa *et al.* (Papa, 1976; Papa *et al.*, 1973) have proposed a cooperative mechanism for proton pumping in respiratory enzymes. By analogy to the cooperative linkage in hemoglobin, known as the Bohr effect (Wyman, 1968; Kilmartin and Rossi-Bernardi, 1973), the redox linkage in cytochromes and the derived cooperative model for proton pumping were denominated redox Bohr effects and vectorial Bohr mechanism, respectively. Redox Bohr effects in cytochromes result in pH dependence of the midpoint potentials (Wilson *et al.*, 1972) and in proton transfer associated to oxido-reduction of the metals (Papa *et al.*, 1986). The H^+/e^- linkage, is likely to arise from modification of the coordination bonds of metal centers associated with change in their valence state. The linkage can involve exchange of axial ligands and p*K* shifts (Wikström *et al.*, 1994; Iwata *et al.*, 1995). The H^+/e^- linkage can also involve porphyrin substituents (Babcock and Callahan, 1983; Woodruff *et al.*, 1991) and conformational propagation of primary effects over long distances in the protein, as in the oxygen Bohr effect of hemoglobin. In the formulation of the vectorial Bohr mechanism the cooperative events were conceived to be extended over the transmembrane span of the protein so as to promote proton uptake from the N aqueous phase and release to the P aqueous phase (Papa, 1976). The vectorial Bohr mechanism thus encompasses by definition cooperative p*K* shifts of ligands of the redox metals as well as p*K* shifts of distant residues in the proton input and proton output pathways (see the case of the light-driven proton pump of bacteriorhodopsin (Henderson *et al.*, 1990).

The "histidine cycle," which has been put forward to explain coupling in cytochrome *c* oxidase between oxido-reduction at the binuclear hema a_3-Cu_B center and proton pumping (Wikström *et al.*, 1994; Iwata *et al.*, 1995), is, in fact, based on redox-linked binding changes at Cu_B of an invariant histidine ligand. The membrane vectorial asymmetry of the proton translocation associated to redox-linked ligand exchange at Cu_B is proposed to be contributed by distinct putative proton conduction pathways detected by x-ray crystallographic analysis of the oxidase (Iwata *et al.*, 1995; Tsukihara *et al.*, 1996). Protolytic events associated with the individual steps of the oxygen reduction to H_2O at the catalytic center have been characterized by different groups (Hallen and Nilson, 1992; Konstantinov *et al.*, 1992; Mitchell *et al.*, 1992; Papa *et al.*, 1994; Rich, 1995).

Analysis in our laboratory of the pH dependence of H^+ transfer associated to redox transitions of the metal centers in cytochrome *c* oxidase, isolated from bovine heart mitochondria, in the soluble and liposome reconstituted state has led us to identify four groups undergoing reversible redox-linked p*K* shifts, attribute their linkage to the individual redox centers (Capitanio *et al.*, 1997a), and to resolve the membrane vectorial nature of the proton transfer (Capitanio *et al.*, 1997b, c; Papa *et al.*, 1998). The results of these investigations have provided direct evidence for involvement of

[1] Institute of Medical Biochemistry and Chemistry, University of Bari, Bari, Italy.

0145-479X/98/0200-0109$15.00/0

redox Bohr effects in the proton pump of cytochrome *c* oxidase.

2. IDENTIFICATION OF THE PROTOLYTIC GROUPS LINKED TO OXIDO-REDUCTION OF HEME *a*, HEME a_3 AND CU_B

Figure 1 summarizes the results of a systematic analysis of the pH dependence of the H^+ transfer associated to redox transitions of the metal centers in the soluble cytochrome *c* oxidase from bovine heart mitochondria, in the unliganded, CN- and CO-liganded state (Capitanio *et al.* 1997a). In the unliganded oxidase the experimental values obtained for the overall H^+/COX ratio of redox Bohr effects increased from about 1 at pH 6.0 to a maximum of 2.7 at alkaline pH values. In the CN-liganded enzyme the H^+/COX ratio exhibited a bell-shaped pH profile with highest ratios of 1.1–1.2 at pH values around 6.8. In the CO-liganded enzyme the H^+/COX ratio also showed a bell-shaped curve but, in this case, the maximum values did not exceed 1.0 and were at pHs around neutrality lower than those measured in the CN-liganded enzyme (see also Mitchell and Rich, 1994). The H^+/COX ratios determined at the various pHs were fitted with functions involving different numbers of protolytic groups. The functions giving the best fits allowed identification of four groups undergoing reversible redox-linked p*K* shifts. Two protolytic groups, with pK_{ox} and pK_{red} values around 7 and $\geq$ 12, respectively, resulted in being linked to redox transitions of heme a_3. One protolytic group with pK_{ox} and pK_{red} values around 6.4 and 7, respectively, is apparently linked to Cu_B (cf. Mitchell and Rich, 1994). The fourth group with pK_{ox} around 6 and pK_{red} around 9 is linked to oxido-reduction of heme *a* (Table I) (Capitanio *et al.* 1997a).

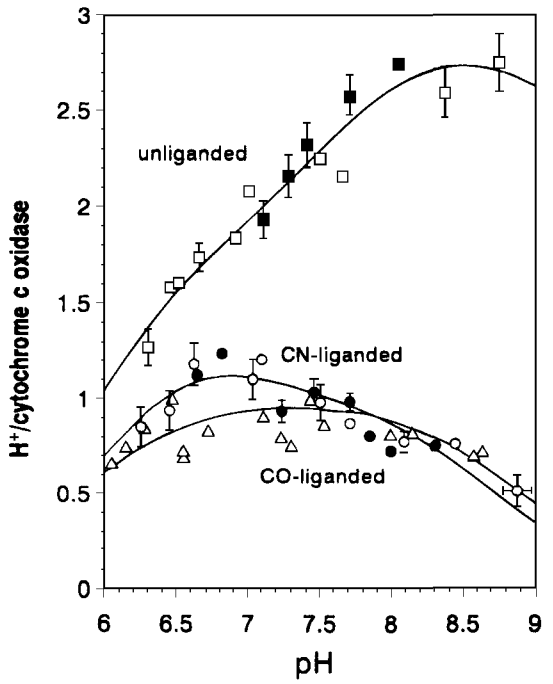

Fig. 1. pH dependence of redox-Bohr effects (H^+/COX coupling number) in soluble cytochrome *c* oxidase. Open and closed squares refer to experiments carried out on the unliganded enzyme using succinate (in the presence of a "catalytic" amount of mitochondria *plus* cytochrome *c*) or ascorbate (in the presence of TMPD plus cytochrome *c*) as reductants, respectively. Open and closed circles refer to experiments with CN-liganded enzyme using succinate or ascorbate as reductants, respectively. Triangles refer to experiments with the CO-liganded enzyme. Where indicated by vertical bars the points represent the mean ± S.E.M. of three or more measurements at the given pH. The curves represent the best-fits analysis of the experimentally determined H^+/COX ratios (see Capitanio *et al.*, 1997a and text for further details).

The assignment of the p*K* shifts of the four protolytic groups to individual metal centers in the oxidase does not exclude the possibility that the p*K* of a single group could also be influenced by cooperative interactions of different metals.

One of the two protolytic groups linked to heme a_3 could be a H_2O molecule ligated to the heme Fe (Mitchell *et al.* 1992). The other, or both, may be protolytic residues in subunit I of the oxidase or in the porphyrin ring of the heme. The group linked to Cu_B with pK_{ox} and pK_{red} values around 6.4 and 7, respectively, could be one of the three histidine ligands (Tsukihara *et al.* 1996) in the imidazole/imidazolium state. This does not support the "histidine cycle," at least in the version based on redox-linked binding change at

Table I. pK Values Obtained from "Best-Fit" Analysis of the pH Dependence of the Measured H^+/COX Ratios for Redox-Linked Scalar H^+ Transfer in Soluble Cytochrome *c* Oxidase[a]

Active redox centers	pK_{ox} ± S.D.	pK_{red} ± S.D.
Heme *a*	6.0±0.2	8.8±0.1
Heme a_3	7.1±0.4	≥ 12
"	7.4±0.4	≥ 12
Cu_B	6.4±0.2	7.0±0.3

[a] The table gives the means of the p*K* values for the four groups calculated from the pH dependence of the experimentally measured H^+/COX ratios in the free and liganded oxidase (from Capitanio *et al.*, 1997a).

CuB of one of the histidine ligands between CuB-bound imidazolate (p$K \approx 14$), imidazole, and free imidazolium. The pK shift of the group linked to CuB appears also to be too small to represent an energetically relevant step in the pump (see under Conclusions for further discussion of this point).

The nature of the group linked to heme *a* remains to be determined. Since this center does not bind O_2, O_2 reduction intermediates, or other ligands, the group in question is likely to be an amino acid in subunit I. Tsukihara *et al.* (1996) have identified, by X-ray crystallography of the bovine heart oxidase, a hydrogen-bond interaction between the hydroxyl group of the farnesyl of heme *a* and subunit I Ser382.

3. THE MEMBRANE VECTORIAL ORGANIZATION OF THE REDOX BOHR EFFECTS

The membrane vectorial organization of the redox Bohr effects has been analyzed in our laboratory by direct measurement of proton transfer associated with oxido-reduction of the metal centers in the cytochrome *c* oxidase from bovine heart reconstituted in liposomes (COV) (Capitanio *et al.* 1997bc).

Figure 2 and Table II show the result with the CO-liganded reconstituted oxidase at pH 7.4. The oxidase was fully reduced by succinate in the presence of a trace of broken mitochondria, cytochrome *c*, and CO. Addition of a small amount of ferricyanide, substoichiometric with the redox metals in the oxidase, gave oxidation of heme *a*, Cu_A, and cytochrome *c;* oxidation of Cu_B and heme a_3 was blocked by CO. The oxidation of heme *a* and Cu_A was accompanied by a synchronous release of H^+ which continued, as expected, during the re-reduction of the metal centers by succinate. The overall reduction of added ferricyanide by succinate should have resulted in 1 to 1 stoichiometric release of H^+ in the external medium. The observed acidification was, however, significantly larger than the amount of ferricyanide added. There is an additional source of H^+ which appears to be associated with the transient oxidation of heme *a;* the oxidation of cytochrome *c* and Cu_A is irrelevant in this respect as they are pH independent (Erecinska *et al.* 1971; Blair *et al.*, 1985). It is thus evident that the Bohr protons associated with the oxidation of heme *a*, and amounting to about 0.9 H^+/COX at pH 7.4 (compare with Fig. 1), are released in the external aqueous phase. If the redox Bohr protons were then taken up by the oxidase from the same external aqueous phase upon re-reduction of heme *a* by succinate, no net excess of H^+ release, with respect to the ferricyanide added, should have been left when heme *a* was fully re-reduced, as was instead observed. The remaining extra-acidification, which was equal to the rapid H^+ release associated with heme *a* oxidation, shows that the Bohr protons associated with re-reduction of heme *a* are taken up from the inner aqueous phase. In the presence of CCCP, which equilibrated the inner and outer pH changes, the same initial rapid acidification was observed upon oxidation of heme *a* by ferricyanide, as in the coupled system, but at the completion of the re-reduction of heme *a* no extra-acidification, with respect to the ferricyanide added, was observed (Fig. 2 and Table II).

The same measurements were then carried out with the reconstituted unliganded oxidase. The oxidation of the metal centers of the oxidase by a substoichiometric amount of ferricyanide resulted at pH 8.2 in the release of 2.17 H^+/COX (Table II) which was very close to the H^+ release corresponding to the Bohr effects associated with oxidation of heme *a* and a_3; at this pH there is no contribution of the Bohr effect of Cu_B (Capitanio *et al.* 1997a). Also in the unliganded oxidase, when re-reduction by succinate of the metal centers of the oxidase was completed, an extra-acidification, with respect to the ferricyanide added, was left. This extra-acidification which amounted to 0.9 H^+/COX was equivalent to that observed with the CO-liganded oxidase and practically corresponded to the Bohr protons associated with heme *a*. It can thus be concluded that both in the unliganded and CO-liganded oxidase the redox Bohr effect linked to heme *a* displays membrane vectorial asymmetry, i.e., protons are taken up by the enzyme from the inner aqueous phase upon reduction of the heme and released in the external aqueous phase upon its oxidation. The observation that the E_m of heme *a* responds to the intramitochondrial pH (Artzatbanov *et al.* 1978) might be related to the membrane asymmetry of the redox Bohr effect linked to heme *a*. The redox Bohr protons linked to heme a_3 appear, on the other hand, to be released in, upon oxidation, and taken up, upon reduction, from the external aqueous space (Table II).

The membrane vectoriality of the redox Bohr effect linked to Cu_B was clarified by analysis of the redox Bohr effects in the unliganded COV at pH 6.7 where the redox Bohr effect for Cu_B reaches the peak of 0.3 H^+/COX (Capitanio *et al.* 1997a). The data obtained at this pH indicate that the Bohr protons

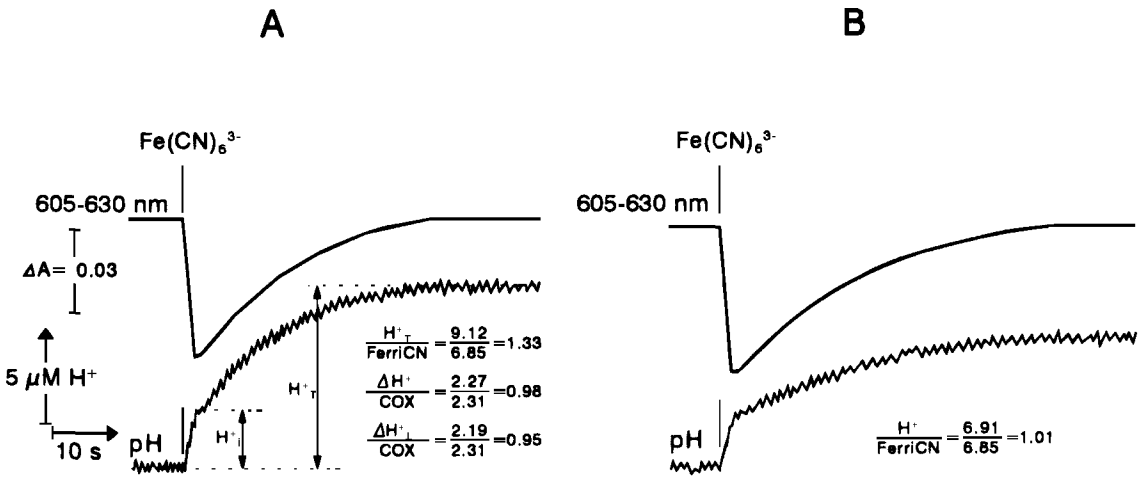

Fig. 2. Analysis of the sidedness of H^+ transfer associated with redox transitions of heme *a* in CO-liganded cytochrome *c* oxidase vesicles. (A) 2.5 μM COV were suspended in 0.15 M KCl and supplemented with 2.5 μM cytochrome *c*, 1 μl/ml valinomycin, and 0.1 mg/ml frozen-thawed beef-heart mitocondria, pH 8.2. The suspension was bubbled with CO for 2 min and then covered with a layer of mineral oil to prevent further gas exchange. Addition of 3 mM succinate produced anaerobiosis and full reduction of cytochrome *c* oxidase in 10–15 min. Where indicated, anaerobic ferricyanide, substoichiometric with respect to the active redox centers, cytochrome *c*, heme *a*, and Cu_A (heme a_3 and Cu_B were clamped in the CO-liganded reduced state) were added and heme *a* absorbance and pH changes monitored simultaneously. Difference spectra collected after addition of succinate showed the characteristics of the fully reduced CO-liganded aa_3 and upon addition of ferricyanide those of the mixed valence CO-liganded aa_3. (B) The same experimental conditions but in the presence of 3 μM CCCP. See text, Table II, and Capitanio *at al.*, 1997b for further details.

linked to oxidation of Cu_B are released, as those of heme *a* and heme a_3 in the external space (see Table II), but are taken up, as those linked to heme *a*, from the inner space upon its re-reduction. This is clearly shown by the fact the extra-acidification observed at the completion of the ferricyanide-induced redox cycle

Table 2. Statistical Analysis of the Sidedness of H^+ Transfer Linked to Redox Transitions of the Metal Centers in Reconstituted Cytochrome *c* Oxidase Vesicles[a]

Experimental conditions	H_T^+ ferricyanide added		ΔH+/COX	H_I^+/COX
	n	Mean ± S.E.		
Co-liganded, pH 7.4				
Coupled	8	1.25 ± 0.02	0.86 ± 0.07	0.90 ± 0.10
Uncoupled	8	0.90 ± 0.05		
Unliganded, pH 8.2				
Coupled	12	1.21 ± 0.02	0.92 ± 0.08	2.17 ± 0.09
Uncoupled	12	1.02 ± 0.01		
Unliganded, pH 6.7				
Coupled	9	1.15 ± 0.01	1.17 ± 0.08	1.60 ± 0.10
Uncoupled	9	0.96 ± 0.03		

[a] For experimental conditions with the CO-liganded and unliganded cytochrome *c* oxidase, see Fig. 2 and Capitanio *at al.*, 1997b. H_T^+/ferricyanide: total amount of H^+ released following the oxidation–reduction cycle elicited by the addition of ferricyanide, divided by the amount of ferricyanide added. Internal measurements showed that the total amount of redox carriers oxidized was equivalent to the amount of ferricyanide added. ΔH+/COX refers under coupled conditions to the ratio between the extra H^+ release with respect to the amount of ferricyanide added and the amount of cytochrome *c* oxidase undergoing oxido-reduction; the difference between the mean values estimated in the unliganded conditions at pH 6.7 and 8.2 was statistically significant ($P < 0.05$). H_I^+/COX refers to the ratio between the initial H^+ release associated to the rapid oxidation of metal centers and the amount of cytochrome *c* oxidase; *n* is the number of the experiments performed.

($\Delta H^+/COX$) was at pH 6.7 larger than at pH 8.2, 1.17 ± 0.08 and 0.92 ± 0.08 ($P<0.05$), respectively, and the difference between these two values practically corresponded to the Bohr protons linked to Cu_B (see Fig. 5 of Capitanio *et al.* 1997a). It can be noted that in the unliganded enzyme the initial acidification (H_i^+/COX) measured upon ferricyanide addition was larger than the extra-acidification ($\Delta H^+/COX$) measured at the end of the redox cycle. The difference between the initial and final extent of acidification practically corresponds to the Bohr protons associated to heme a_3 which are released in, upon oxidation, and taken up, upon re-reduction, from the external aqueous phase.

The analysis of the vectorial nature of the redox-linked proton transfer in COV shows that the proton transfer resulting from the redox Bohr effects linked to heme *a* and Cu_B in the bovine heart cytochrome *c* oxidase displays membrane vectorial asymmetry, i.e., protons are taken up from the inner aqueous space, upon reduction, and released in the external space, upon oxidation of the metals (Fig, 3). This direction of the proton uptake and release is just what is expected from a vectorial Bohr mechanism in which redox-linked cooperative events are conceived to be extended over the transmembrane span of the enzyme so as to result in proton uptake from the inner and their release in the external aqueous phase (Papa, 1976).

The two groups whose p*K*'s change upon oxido-reduction of heme a_3 exchange protons only with the external aqueous phase (Fig. 3). This would exclude a role of these two groups in proton pumping. The group linked to heme *a*, whose p*K* changes upon reduction from 6 to around 9 and which can transfer up to 0.9 H^+ per e^-, should provide the major contribution to the proton pump. The possible involvement in proton pumping of protolytic groups linked to heme *a* has already been entertained by others. Based on resonance Raman spectroscopy involvement of a (tyrosine) residue hydrogen-bonded to the carbonyl group of the formyl substituent of heme *a* (Babcock and Callahan, 1983) and of residue(s) near to and with p*K* shifts linked to heme *a*, exchanging protons with a H_2O molecule close to the formyl substituent of heme *a* has been proposed (Rousseau *et al.* 1988; cf. Wikström, 1982). The group linked to Cu_B undergoes, upon reduction, only a small increase in its p*K*, from 6.4 to 7.0, and consequently does not transfer more than 0.3 H^+ per e^- (at pH 6.7).

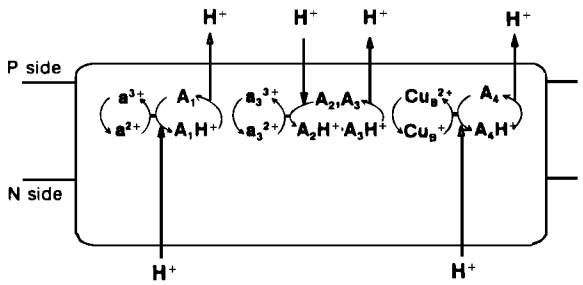

Fig. 3. Membrane sidedness of Bohr protons linked to oxido-reduction of hemes *a*, a_3 and Cu_B. For details see Fig. 2, Table II, and text.

4. FEATURES OF PROTON PUMPING AND ROLE OF HEME *a*

There are features of the proton pump of cytochrome *c* oxidase which appear to be consistent with a critical role of heme *a* in this process. These are represented by the pH dependence of the H^+/e^- ratio observed in COV and by the variability of the H^+/e^- ratio under the influence of the rate of electron flow in the oxidase and the transmembrane ΔpH (Papa *et al.* 1987, 1994; Capitanio *et al.* 1996).

The results summarized in Fig. 4 show that the H^+/e^- ratio for proton ejection driven by ferrocytoch-

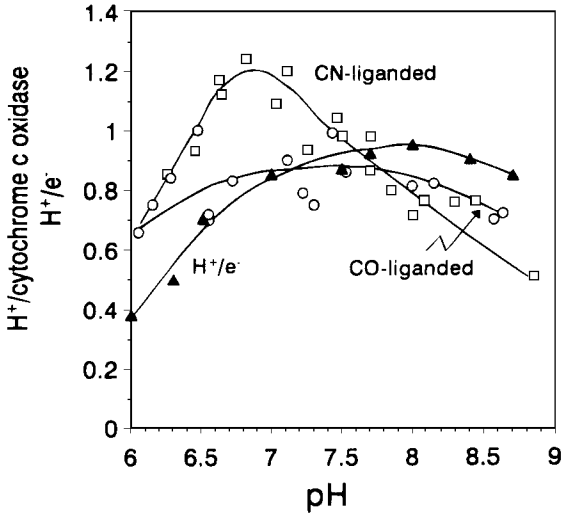

Fig. 4. Comparison between pH dependence of the redox-linked proton pump stoicheiometry and that of redox-Bohr effects (H^+/COX coupling number) in cytochrome *c* oxidase. The H^+/e^- ratio of the proton pump (closed triangles) was determined by the ferrocytochrome *c* pulse method in cytochrome *c* oxidase vesicles (from Papa *et al.*, 1987). The H^+/COX coupling numbers with their best-fit curves refer to the redox-Bohr effects measured in CN- and CO-liganded (open squares and circles, respectively) soluble cytochrome *c* oxidase, see Fig. 1.

rome *c* oxidation in COV increases with pH, up to about one at pH's around 8 and then declines at higher pH's (Papa *et al.* 1987). When compared with the pH-dependence of redox Bohr effects in the soluble oxidase, the curve for the pH dependence of the H^+/e^- ratio for proton pumping appears to be similar to that observed for the H^+/COX ratio of the Bohr effect in the CO-liganded oxidase, which is linked to oxido-reduction of heme *a*. The pH dependence curve for the H^+/COX ratio of the redox Bohr effects in the CN-liganded oxidase diverges, on the other hand, from the curves of both H^+ pumping and the Bohr effect linked to heme *a* (CO-liganded oxidase) for a peak around pH 6.9, which is attributed to Cu_B (Capitanio *et al.* 1997a). It should, however, be pointed out that comparison of pH dependence curves for activities of redox enzymes in the soluble and membrane associated state is to be taken with caution.

An extensive study of the influence of kinetic and thermodynamic factors on the H^+/e^- stoichiometry of cytochrome *c* oxidase has been carried out in our laboratory (Papa *et al.* 1991; Capitanio *et al.* 1991, 1996). Accurate measurement of the initial rates of electron flow and proton ejection at level flow have shown that the H^+/e^- ratio of proton pumping by the oxidase varies, both in intact mitochondria and the isolated-reconstituted oxidase from zero at extremes of low and high rates to about one at intermediate rates. This rate-dependence of the output efficiency of the pump in the oxidase is clearly shown by the curve of the H^+/e^- ratios vs the T.N. of the oxidase in Fig. 5. This shows that the values of the H^+/e^- ratio determined in intact mitochondria and COV, in experiments repeated at distance of years and using different electron delivery systems, are all fitted by a single bell-shaped curve.

It has to be mentioned that numerous measurements of the H^+/e^- stoicheiometry in COV have been carried out in different laboratories using the reductant pulse method. In this technique, in which aerobic COV are pulsed with a molar excess of ferrocytochrome *c*, "optimal experimental conditions" are generally used which give H^+/e^- ratios approaching 1 (Wikström and Krab, 1979; Nicholls and Wriggelsworth, 1982; Proteau *et al.* 1983, Papa *et al.* 1987). With the pulse technique the H^+/e^- ratio varies with the pH, the ionic composition of the medium, and the modalities of activation of electron flow (Proteau *et al.* 1983; Papa *et al.* 1987). In any event the prevailing conditions used in the pulse method are such that this technique

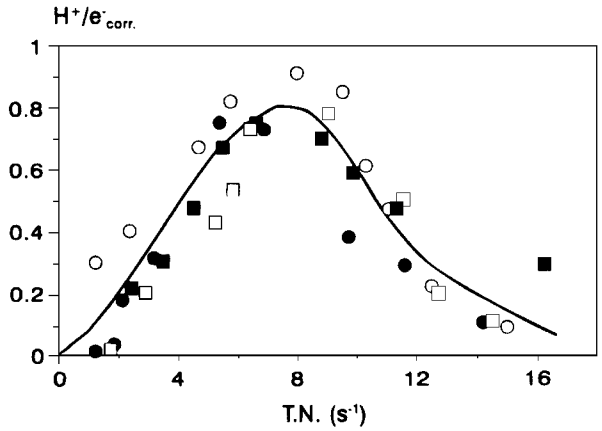

Fig. 5. Dependence of the H^+/e^- ratio of the proton pump on the rate of electron flow in cytochrome *c* oxidase in intact mitochondria and in cytochrome *c* oxidase vesicles (COV) measured under level flow conditions. Rat-liver mitochondria: closed circles: electron flow rate from succinate to oxygen, adjusted with malonate; open circles: respiratory rate with ascorbate, adjusted varying the concentration of TMPD. For details see Papa *et al.* (1991). Cytochrome *c* oxidase vesicles: closed squares: electron flow rate from ascorbate *plus* TMPD supplemented with cytochrome *c*, varied changing the concentration of ferricytochrome *c*; open squares: respiratory rate fueled by duroquinol in the presence of a trace of soluble cytochrome *c* reductase supplemented with cytochrome *c*, changed varying the concentration of cytochrome *c* reductase. Valinomycin (*plus* K^+) was present to collapse aerobic $\Delta\Psi$. The points of all the curves represent the mean of six or more experiments (Capitanio *et al.*, 1996). Level flow measurements, i.e., the H^+/e^- ratios were obtained from the initial rates elicited by the addition of the substrates.

does not provide information on the aspects dealt with systematically in the studies with the rate method.

It seems to be agreed that, in order to be coupled to proton pumping in the oxidase, electron flow has to follow the sequence cyt.$c \rightarrow Cu_A \rightarrow$heme $a \rightarrow$heme a_3-Cu_B (Babcock and Wikström, 1992) (Fig. 6). The a_3-Cu_B binuclear center is the site where the oxygen reduction chemistry takes place and this process is considered to be directly coupled to H^+ pumping (Babcock and Wikström, 1992; Wikström *et al.* 1994; Rich, 1995; Iwata *et al.* 1995). A breakthrough toward the understanding of the molecular mechanism of protonmotive catalysis in cytochrome *c* oxidase is provided by the crystallographic resolution of the structures of cytochrome *c* oxidase from *Paracoccus denitrificans* (Iwata *et al.* 1995) and bovine heart mitochondria (Tsukihara *et al.* 1995,1996). The crystallographic structures, which confirmed predictions based on mutational analysis of the prokaryotic oxidases (Ferguson-Miller, 1993), show that the heme *a* and heme a_3-Cu_B binuclear center are bound in subunit I to histidine residues of transmembrane helices II, X,

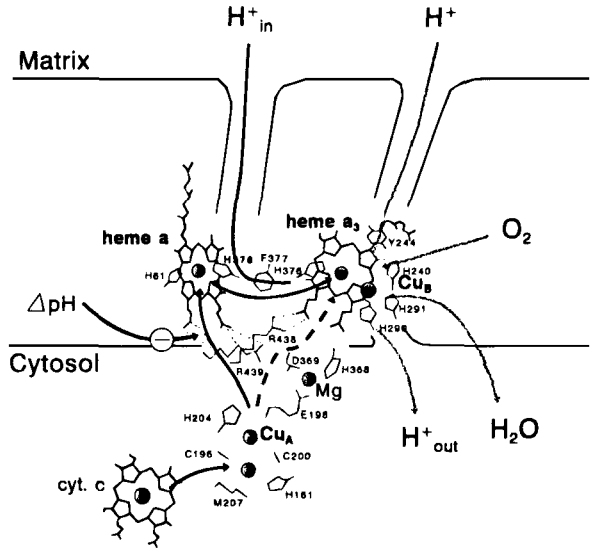

Fig. 6. Sequence of electron transfer steps in cytochrome *c* oxidase. Proton-coupled electron transfer steps are shown by black arrows, decoupled electron transfer (slip) by dashed black arrow. Pathways for pumped protons are shown by black arrows, those for scalar proton transfer by gray arrows. The structure and arrangement of the metal centers and associated residues is drawn from Tsukihara *et al.* (1996). For details see text.

VI, and VII in region extending toward the cytosolic surface (Fig. 6). The propionate groups of both hems *a* and a_3, which are perpendicular to the plane of the membrane, point toward and communicate, through conserved residues in subunit I, with the C-terminal domain of subunit II holding the two cupper atoms of the Cu_A center (Iwata *et al.* 1995; Tsukihara *et al.* 1995,1996). Residues have been located in subunit II and subunit I which can provide a hydrogen bond/ion pair network serving as electron transfer path between Cu_A and heme *a*. In this network His204, a Cu_A ligand in subunit II, is hydrogen bonded to Arg 438 and Arg 439 (bovine numbering) in the loop XI–XII of subunit I; the latter are bonded to the propionate groups of heme *a*. Tsukihara *et al.* (1996) have also identified in the bovine heart oxidase a hydrogen bond network involving the propionate groups of heme a_3, Arg 438 in the loop XI–XII, and His 368 of subunit I, the latter coordinated by Mg^{2+} to Glu 198 in subunit II which is liganded to the lower Cu_A atom. This network could provide direct electron transfer from Cu_A to the heme a_3-Cu_B center (Tsukihara *et al.*, 1996). The distance from the lower Cu_A to heme *a* Fe is some 2Å shorter than that to the heme a_3 Fe. It has been pointed out (H. Michel, personal communication) that with this difference the rate of electron transfer from Cu_A to heme *a* would be much faster than to heme a_3, as suggested by kinetic data (Hill, 1994). Tsukihara *et al.* (1996) think, however, that the structural and kinetic data can yet be compatible with electron transfer from Cu_A to heme *a* as well as to heme a_3. It should be noted that the Cu_A center resides in a different subunit from that holding hemes *a* and a_3. The distances between Cu_A and the two hemes have been measured in the oxidized enzyme. It is conceivable that in the oxidase turning over in the steady state the contacts between subunits I and II and hence the distance between Cu_A and heme *a* and a_3 can be changed. In particular the steady-state $\Delta\mu H^+$ might affect these intersubunit distances.

Combining the structural information with the finding of a variable H^+/e^- stoichiometry, our group has proposed that electron transfer from Cu_A to the heme a_3-Cu_B center can take place along two pathways (Fig. 6) (Papa *et al.* 1994; Capitanio *et al.* 1996). The first via heme *a* will be associated through cooperative linkage (redox Bohr effect) to proton pumping. The second pathway will consist of direct electron transfer from Cu_A to the binuclear a_3-Cu_B center, bypassing heme *a* and resulting in decoupling of the proton pump. The occurrence of these two electron-transfer pathways is supported by the observation that in the various states of the respiratory proton pump in COV, the reduction level of Cu_A is found to be lower than that of heme *a* and is enhanced less than that of heme *a* by raising the rate of electron delivery to the oxidase (Capitanio *et al.* 1996). The actual H^+/e^- in the oxidase will be determined by the relative contribution of the two-electron transfer pathways and can vary from a maximum of 1 to 0 (Papa *et al.* 1994). The relative contribution of the two pathways can be dictated by kinetic and thermodynamic factors. Under level flow conditions, the H^+/e^- ratio should only be influenced by kinetic factors. At initial rates below 4 electrons $\cdot$ $sec^{-1} \cdot aa_3^{-1}$ the H^+/e^- ratio approaches 0. This might reflect the fact that in order to perform proton pumping, the oxidase has to experience a full turnover with the passage of 4 electrons/mole of aa_3 (Babcock and Wikström, 1992). With enhancement of the rate of electron flow, the H^+/e^- ratio increases and, at intermediate rates, tends to the maximal obtainable value. The kinetic situation could be adjusted here to have the electron flowing almost exclusively through the coupled pathway via heme *a*. As the electron pressure and the rate of electron transfer in the oxidase are further increased, the decoupled electron transfer pathways, directly from Cu_A to the binuclear center, can start to

become more important with a decrease in the H^+/e^- stoichiometry. The atomic resolution of the structure of cytochrome *c* oxidase provided by the X-ray crystallographic analyses now offers the basis for site directed mutational analysis to verify the proposed occurrence of the two pathways for electron transfer from Cu_A to the binuclear a_3-Cu_B center.

Proton pumping in cytochrome *c* oxidase, as well as in the bc_1 complex, is at the steady state, partially decoupled by the ΔpH component of Δ*p* (Lorusso *et al.* 1995; Capitanio *et al.* 1996). This decoupling should not be confused with the δ*p*-dependent membrane leak. Promotion of the steady-state proton leak by a protonophore, which decreases the ΔpH, has been shown to alleviate ΔpH-dependent slip in both bc_1 vesicles and COV (Cocco *et al.* 1992; Capitanio *et al.* 1996). At the steady state, alkalinization of the N phase can result in proton slip due to loss of the protonation asymmetry of the critical protolytic group(s) in the pump in the input state. This protonation step might have a limited kinetic capacity (Hallen and Nilson, 1992; Hallen *et al.* 1994).

In the case of cytochrome *c* oxidase δpH can exert an additional decoupling effect by exerting an inhibitory back pressure on the proton-coupled electron transfer from Cu_A to the a_3-Cu_B center via heme *a* without, obviously, affecting the putative decoupled electron transfer directly from Cu_A to the binuclear center.

It should be noted that the loss of energy conversion effected in the proton pump by ΔpH, and in the oxidase also by high respiratory rates, is alleviated in mitochondria by: (i) direct Δ*p* generation from the membrane anisotropy of the reduction of O_2 to H_2O in the oxidase, (ii) proton-coupled uptake of phosphate and respiratory substrates, (iii) proton influx for ATP synthesis in phosphorylating mitochondria which all contribute to prevent establishment of a large ΔpH so that proton pumping at the steady state can be preserved.

5. CONCLUSIONS

Figure 7 describes the putative steps of proton translocation associated with the reduction of dioxygen to H_2O by ferrocytochrome *c* in the oxidase. Transfer via *heme a* of each of the four electrons from Cu_A to the binuclear a_3-Cu_B center is associated with uptake of protons from the N aqueous phase and their translocation toward the P side of the membrane. Coupling

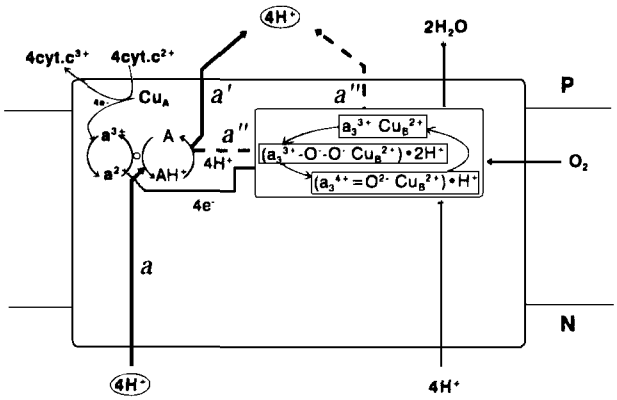

Fig. 7. A cooperative proton pump model in cytochrome *c* oxidase with the involvement of the vectorial Bohr effect linked to heme *a*. The thick black arrows (pathway *a*-*a'*) show the vectorial proton translocation in cytochrome *c* oxidase provided by the anisotropic H^+ transfer of a protolytic group linked to redox transitions of heme *a*, with H^+ uptake from the N side upon reduction of heme *a* and H^+ release at the P side upon its oxidation. The dashed black arrow shows the protonmotive activity of the enzyme provided by combination of the redox-Bohr effect of heme *a* and protonmotive events associated to the chemistry of dioxygen reduction at the heme a_3-Cu_B binuclear center (pathway *a*-*a''*). Bohr protons released upon oxidation of heme *a* are transferred to the binuclear center where the P, F, and O intermediates are formed (see text) and from there translocated to the P side when scalar protons, taken up from the N side, compensate the negative charges of the intermediates of oxygen reduction (cf. Wikstrom *et al.*, 1994; Rich, 1995).

of proton translocation to electron transfer via heme *a* is afforded by the Bohr effect linked to oxido-reduction of this heme and could take place, at least for a part of its route, along the proton-conducting hydrogen-bond network seen in the crystal structure of the bovine oxidase to be contributed by residues of transmembrane helices XI and XII of subunit I with intercalated H_2O molecules (Tsukihara *et al.*, 1996) (Fig. 8). Resonance Raman spectroscopy has revealed the presence near heme *a* of H_2O molecules which could be involved in proton translocation (Rousseau *et al.*, 1988). It has been proposed that proton transfer by the above pathway can be controlled by redox transitions of heme *a*, as the OH group of the farnesyl chain of the porphyrin is hydrogen-bonded to Ser832 in the proton pathway (Tsukihara *et al.*, 1996).

The packing of helices XI and XII, which would be essential for proton pumping, can be stabilized by the interaction at the N-surface of the membrane of the C-terminus of subunit I with the peripheral loop connecting its helices II and III and the N-termini of subunits IV and VIII (Papa *et al.*, 1998). The decoupling of the pump observed upon proteolytic cleavage

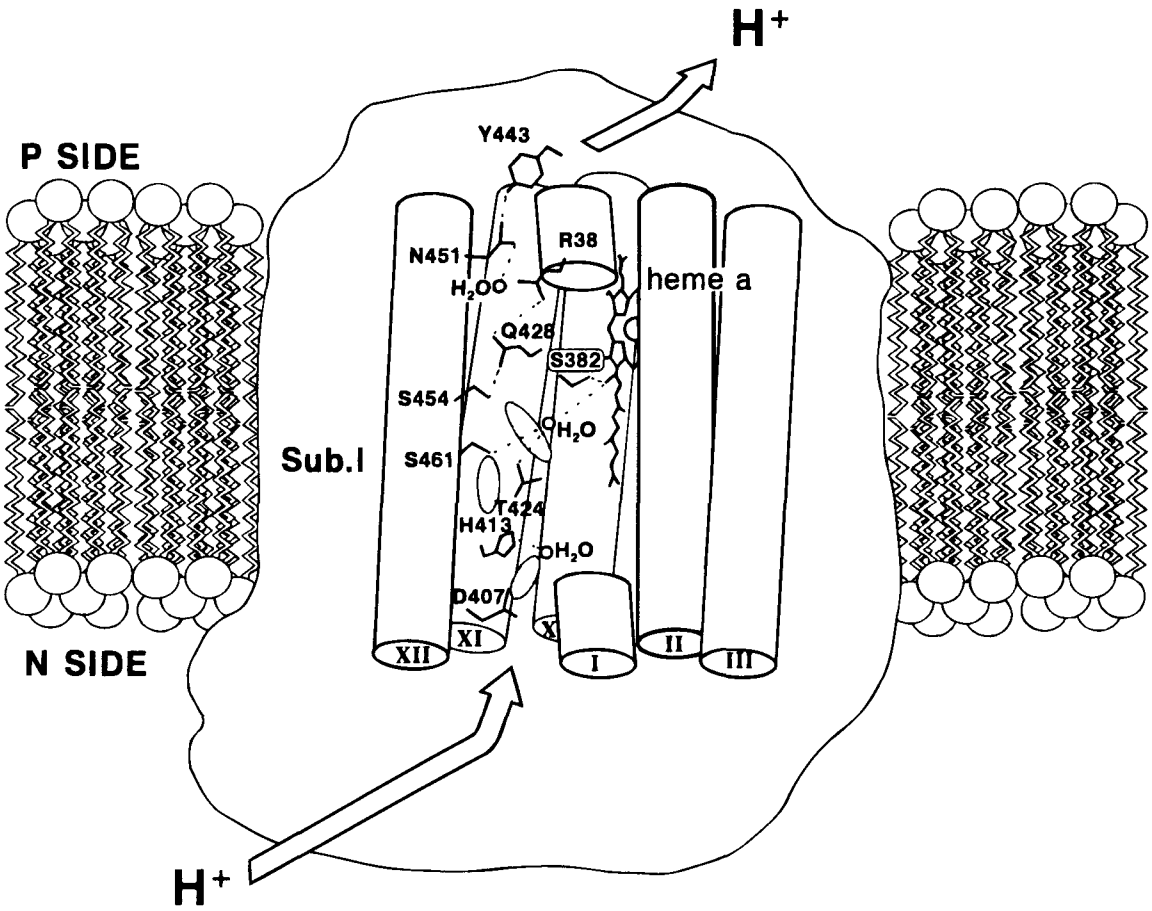

Fig. 8. Schematic representation of a possible channel for proton pumping in cytochrome *c* oxidase. The drawing is based on the structural information derived from X-ray difraction analysis of bovine heart cytochrome *c* oxidase crystal (Tsukihara *et al.*, 1996). Gray ovals and dotted lines denote internal cavities possibly occupied by H_2O molecules and hydrogen bonds, respectively.

of the hydrophylic N-terminus of subunit IV (Capitanio *et al.*, 1994) would, thus, support the involvement of the above hydrogen-bond network in proton pumping. This would also be consistent with the finding that mutation of Asp91 in the loop connecting helices II and III results in decoupling of the proton pump in prokaryotic heme-copper oxidases (Thomas *et al.*, 1993; Fetter *et al.*, 1995).

Of the various intermediate steps in the four-electron reduction of dioxygen to water, those resulting from the utilization of the third and fourth electron, i.e., the reductive cleavage of the peroxy intermediate to the ferryl compound and H_2O and the reduction of the latter to the oxidized enzyme and H_2O, are those associated with the largest free energy release and are considered to provide the energy input for proton pumping (Babcock and Wikström, 1992). One can think of two possible mechanism to combine the heme *a*-linked proton translocation with the redox catalysis at the binuclear center. The first (arrows *a* and *a'* in Fig. 7) is that proton pumping provided by the vectorial Bohr effect linked to heme *a* is only indirectly coupled to the oxygen reduction chemistry at the binuclear center through cooperative interaction of redox events at this center and protonmotive electron transfer by heme *a*. It can be noted that in this case the transfer in the oxidase of each one of the four electrons used in the reduction of O_2 to H_2O can result in the pumping of up to about 1 H^+/e^- (at pHs around 7.4). Evidence has, however, been presented which indicates that only the transfer of the third and the fourth electron is associated with transmembrane pumping of 2 H^+ *per* each one of these two electrons (Wikström, 1989). If this is the case, one might have to consider the alternative possibility that in the turning-over enzyme the protons associated with the transfer by heme *a* of the

electrons to heme a_3 and Cu_B reach and are held in the environment of the binuclear center (arrows *a* and *a''* dotted in Fig. 7) (see Wikström *et al.*, 1998) by electrostatic attraction of negatively charged intermediates until the electronegativity of the two oxide molecules produced in these two steps is neutralized (Rich 1995) by proton translocation by the scalar proton pathway identified in the crystal structure of the *Paracoccus denitrificans* oxidase (Iwata *et al.*, 1995). With the loss of the electrostatic attraction the four protons held at the binuclear center, two each in the P→F and F→O transition, are finally released in the P aqueous phase (Wikström 1989).

In both the alternatives presented in Fig. 7 Cu_B would quantitatively contribute by a small measure to proton pumping as compared to heme *a*. The Cu_B linked group can only contribute up to a maximum of 0.3 H^+/e^- at pH 6.7; at pH 7.4 and higher no redox-linked H^+ transfer by the Cu_B linked group takes place (Capitanio *et al.*, 1997a). This seems to contrast with the "histidine cycle," according to which the overall pumping of 4 H^+ per dioxygen reduced to 2 H_2O is accomplished by histidine shuttling at Cu_B.

We would, however, like to point out that information derived from the pH dependence of scalar proton transfer linked to oxidoreduction of a metal center (redox Bohr effect) in the soluble enzyme might not be directly applicable to its contribution to proton pumping by the enzyme in the membrane where the bulk phase and localized components of the electrochemical proton gradient can influence the protolytic activity of the group(s) involved.

ACKNOWLEDGMENTS

This work was supported by Grant No. 96.03707.CT14 of the Biotechnology Committee of the Italian Council of Research and by a grant of the Italian Project for Supermolecular Systems of MURST, Italy,

REFERENCES

Artzatbanov, V. Y., Konstantinov, A. A., and Skulacev, V. P. (1978). *FEBS Lett.* **87**, 180–185.

Babcock, G. T., and Callahan, P. M. (1983). *Biochemistry* **22**, 2314–2319.

Babcock, G. T., and Wikstrom, M. (1992). *Nature* **356**, 301–309.

Blair, D. F., Ellis, W. R., Wang, H., Gray, H. B., and Chan, S. I. (1985). *J. Biol. Chem.* **261**, 11524–11537.

Capitanio, N., Capitanio, G., De Nitto, E., Villani, G. and Papa, S. (1991). *FEBS Lett.* **288**, 179–182.

Capitanio, N., Peccarisi, R., Capitanio, G.; Villani, G., De Nitto, E., Scacco, S., and Papa, S. (1994). *Biochemistry* **33**, 12521–12526.

Capitanio, N., Capitanio, G., Demarinis, D. A., De Nitto, E., Massari, S., and Papa, S. (1996). *Biochemistry* **35**, 10800–10806.

Capitanio, N., Vygodina T. V., Capitanio, G., Konstantinov, A. A., Nicholls, P., and Papa, S. (1997a). *Biochim. Biophys. Acta* **1318**, 255–265.

Capitanio, N., Capitanio, G., De Nitto, E., and Papa, S. (1997b). *FEBS Lett.*, in press.

Capitanio, N., Capitanio, G., De Nitto, E., and Papa, S. (1997c). Ital. Biochem. Soc. Trans. (IBST) Vol. 8, in press.

Cocco, T., Lorusso, M., Di Paola, M., Minuto, M., and Papa, S. (1992). *Eur. J. Biochem.* **209**, 475–481.

Erecinska, M., Chance, B., and Wilson, D. F. (1971). *FEBS Lett.* **19**, 284–286.

Fergusson-Miller, S. (1993). *J. Bioenerg. Biomembr.* **25**, 167–188.

Fetter, J. R., Qian, J., Shapleigh, J., Thomas, J. W., Garcia-Horsman, A., Schmidt, E., Hosler, J., Babcock, G. T., Gennis, R. B., and Ferguson-Miller, S. (1995). *Proc. Natl. Acad. Sci. USA* **92**, 1604–1608.

Hallen, S., and Nilsson, T. (1992). *Biochemistry* **31**, 11853–11859.

Hallen, S., Brzezinski, P., and Malmstrom, B. G. (1994). *Biochemistry* **33**, 1467–1472.

Henderson, R., Baldwin, J. M., Ceska, T. A., Zemlin, F., Beckman, E., and Downing, K. H. (1990). *J. Mol. Biol.* **213**, 899–929.

Hill, B. C. (1994). *J. Biol. Chem.* **269**, 2419–2425.

Iwata, S., Ostermeier, C., Ludwing, B., and Michel, H. (1995). *Nature* **376**, 660–669.

Kilmartin, J. V., and Rossi-Bernardi, L. (1973). *Physiol. Rev.* **53**, 836–888.

Konstantinov, A. A., Capitanio, N., Vygodina, T. V., and Papa, S. (1992). *FEBS Lett.* **312**, 71–74.

Lorusso, M., Cocco, T., Minuto, M., Capitanio, N., and Papa, S. (1995). *J. Bioenerg. Biomembr.* **27**, 101–108.

Mitchell, R., Mitchell, P., and Rich, P. R. (1992). *Biochim. Biophys. Acta* **1101**, 188–191.

Mitchell, R., and Rich, P. R. (1994). *Biochim. Biophys. Acta* **1186**, 19–26.

Nicholls, P., and Wrigglesworth, J. M. (1982). In: *Oxidase and Related Redox Systems* (King, T. E., *et al.*, eds.) Pergamon Press, New York, pp. 1149–1160.

Papa, S. (1976). *Biochim. Biophys. Acta* **456**, 39–84.

Papa, S., Guerrieri, F., Lorusso, M., and Simone, S. (1973). *Biochemie* **55**, 703–716.

Papa, S., Guerrieri, F., and Izzo, G. (1986). *Methods Enzymol.* **126**, 331–343.

Papa, S., Capitanio, N., and De Nitto, E. (1987). *Eur. J. Biochem.* **164**, 507–516.

Papa, S., Capitanio, N., Capitanio, G., De Nitto, E., and Minuto, M. (1991). *FEBS Lett.* **288**, 183–186.

Papa, S., Lorusso, M., and Capitanio, N. (1994). *J. Bioenerg. Biomembr.* **26**, 609–617.

Papa, S., Capitanio, N., and Villani G. (1998). In *Frontiers of Cellular Bioenergetics: Molecular Biology, Biochemistry, and Physiopathology* (Papa, S., *et al.*, eds.), Plenum Press, London, New York, in press.

Proteau, G., Wrigglesworth, J. M., and Nicholls, P. (1983). *Biochem. J.* **210**, 199–205.

Rich, P. R. (1995). *Aust. J. Plant Physiol.* **22**, 479–486.

Rousseau, D. L., Sassaroli, M., Dhin, Y- C. and Dasgupta, S. (1988). *Ann. N.Y. Acad. Sci.* **550**, 223–237.

Thomas, J. W., Puustinen, A., Alben, J. O., Gennis, R. B., and Wikstrom, M. (1993). *Biochemistry* **32**, 10923–10928.

Tsukihara, T., Aoyama, H., Yamashila, E., Tomizaki, T., Yamagushi, H., Shinzawa-Itoh, K., Nakashima, R., Yaono, R., and Yoshikawa, S. (1995). *Science* **269**, 1069–1074.

Tsukihara, T., Aoyama, H., Yamashila, E., Tomizaki, T., Yamagushi, H., Shinzawa-Itoh, K., Nakashima, R., Yaono, R., and Yoshikawa, S. (1996). *Science* **272**, 1136–1144.

Wikstrom, M. (1982). In *Electron Transport and Oxygen Utilization* (Ho, C., (ed.), Elsevier-North Holland, New York, pp. 271–277.

Wikstrom, M. (1989). *Nature* **338**, 776–778.

Wikstrom, M., and Krab, K. (1979). *Biochim. Biophys. Acta* **549**, 177–222.

Wikstrom, M., Morgan, J. E., Hummer, G., Woodruff, W. H., and Verkhovsky, M. I. (1988). In *Frontiers of Cellular Bioenergetics: Molecular Biology, Biochemistry and Physiopathology* (Papa, S., *et al.*, eds.), Plenum Press, London, New York, in press.

Wikstrom, M., Bogachev, A., Finel, M., Morgan, J. E., Puustinen, A., Raitio, M., Verkhovskaya, M., and Verkhovsky, M. I. (1994). *Biochim. Biophys. Acta* **1187**, 106–111.

Wilson, D. F., Lindsay, J. G., and Brocklehurst, E. S. (1972). *Biochim. Biophys. Acta* **256**, 277–286.

Woodruff, W. H., Einarsdottir, O., Dyer, R. B., Bagley, K. A., Palmer, G., Atherton, S. J., Goldbeck, R. A., Dawes, T. O., and Kliger, D. S. (1991). *Proc. Natl. Acad. Sci. USA* **88**, 2588–2592.

Wyman, J. (1968). *Quat. Rev. Biophys.* **1**, 35–80.